Engineering Failure Analysis 90 (2018) 90–102

Contents lists available at ScienceDirect

Engineering Failure Analysis

journal homepage: www.elsevier.com/locate/engfailanal

The effects of degassing, grain refinement & Sr-addition on melt quality-hot tear sensitivity relationships in cast A380 aluminum alloy

Muhammet Uludağ[a,*], Remzi Çetin[b], Derya Dispinar[c], Murat Tiryakioğlu[d]

[a] Department of Metallurgical and Materials Engineering, Faculty of Natural Sciences, Architecture and Engineering, Bursa Technical University, Bursa, Turkey
[b] Faculty of Engineering, KTO Karatay University, Konya, Turkey
[c] Faculty of Engineering, Istanbul University, Istanbul, Turkey
[d] School of Engineering, University of North Florida, Jacksonville, FL 32224, USA

ARTICLE INFO

Keywords:
Degassing
Grain refinement
Modification
Bifilms
Hot tearing

ABSTRACT

Hot tearing tendency of A380 with various element additions (Sr, Sr + Ti, Ti, B and B + Sr) was investigated. Constrained rod casting (CRC) hot tearing test method was used to characterize the hot tearing sensitivity. Reduced pressure test (RPT) samples were produced from each condition and all trials were repeated three times. Number density of pores on the cross section of RPT samples was calculated via digital image processing and statistical analysis was carried out. Microstructure analysis was carried out to observe the effect of alloying elements. Hot torn cross sections were subjected to SEM analysis. It was found that in aluminum alloys, the most deleterious defects, bifilms that are the cause of many defects, play an important role in initiating the hot tearing during solidification. It is important to note that the shape, size and distribution of bifilms are too complex. They act as heterogeneous nucleation site for liquid to separate and thus increase hot tearing.

1. Introduction

Surface of most liquid metals is covered by a film that forms as a result of the reaction of atmosphere with the metal. These films are harmless as long as they remain on the surface. However, they can be entrained into the bulk of the melt when the surface is disturbed, such as with additions to the melt, and/or when new surfaces are created, such as during pouring. These entrained films are called bifilms because of their double, film-on-film nature [1]. In aluminum alloys, they remain in the liquid and have a deleterious effect on casting quality, mechanical properties and performance of castings. To produce high quality aluminum castings, it is essential to start with a melt that is substantially free from bifilms and bifilm-opening agents such as hydrogen dissolved in liquid aluminum and intermetallics such as Fe-containing phases [2]. If the initial melt quality is too low that a good casting cannot be made from it, it is fruitless to use the best practices in filling and feeding of castings. Conversely high quality melts can be damaged significantly when surface oxide films are entrained into the casting during melt transfers and in poorly-designed filling systems.

When initial melt quality is poor and/or significant damage is given to liquid metal, casting suffers from defects, such as pores, inclusions and hot tears. Although pores and hot tears have been traditionally regarded as intrinsic defects [3], i.e., occurring as a result of metal properties, recent research [1] has shown that the root cause of pores and hot tears are bifilms. Moreover in situ

* Corresponding author.
E-mail address: muhammet.uludag@btu.edu.tr (M. Uludağ).

https://doi.org/10.1016/j.engfailanal.2018.03.025
Received 19 October 2017; Received in revised form 14 March 2018; Accepted 15 March 2018
Available online 16 March 2018

experiments with solidifying transparent liquids have shown that hot tears are initiated by pores or inclusions.

Although the effect of melt additions and processing parameters on hot tear sensitivity has been studied in the literature, there has not been a study in which the combined effect of degassing, grain refining and Sr-modification on initial melt quality as well as its correlation with hot tear sensitivity have been investigated simultaneously, to the authors' knowledge. This study is motivated by this gap in the literature.

2. Background

2.1. Melt quality

Strontium is added to Al-Si alloys so that the morphology of Si eutectic changes from acicular to fibrous with the intention of improving mechanical properties [4–8]. However, Sr additions have been reported [9] to increase porosity in Al castings. Some users have even reported that the increased porosity more than negates any beneficial effects of Sr, and consequently they abandoned modification by Sr [10–12]. Bifilms in the melt and Sr additions interact to initiate pores in Al-Si alloys [13–15]. Iwahori et al. [14] investigated the effect of Sr additions on porosity in Al-7%Si alloys and reported that whether Sr additions result in porosity depended on the number of oxides in the melt. When entrained oxide content was low, Sr additions combined with vacuum degassing did not lead to porosity. With high level of entrained oxides, degassing combined with Sr addition increased porosity. Argo and Gruzleski [16] investigated the effect of Sr modification on how A356 alloy shrank during solidification by using the Tatur test. In unmodified alloys, metal created a larger central shrinkage pipe and low level of internal microshrinkage. After Sr addition, the size of the central pipe got smaller but the internal microshrinkage level increased. Similar results were reported [17] for an Al-9%Si alloy. Tiedje et al. [18,19] investigated the effect of Sr modification and cooling rate on size and distribution of porosity in Al-7%Si and Al-12%Si alloys and observed that pore area and number of pores per unit area, i.e., number density (N) increased after Sr addition. Similar results were found by Liao et al. [20] who investigated the effect of Sr concentration on the amount of porosity in Al-12.3%Si alloy. Sr modification increased both N and volume fraction of porosity. Roy et al. [21] found that Sr additions to melts of an Al-9%Si-3%Cu alloy increased N and distributed them evenly in the casting. Liu et al. [22] found that Sr additions to A356 and 319 cast aluminum alloys increased porosity and resulted in the formation of Al_2SrO_3 oxide, which served as initiation sites for pores. Rotary degassing with Ar was essentially ineffective in removing these oxides [23]. The results in the literature show that Sr addition increases the number of bifilms in the melt. These bifilms are probably much finer than the “old” oxides that used to be the skin of the ingot or the remelts. That is why they are efficient in redistributing porosity and making pores finer.

In aluminum alloys, Al-Ti-B grain refiners are added to alter the coarse α-Al to finer dendrites. Anyalebechi [24] reported that grain refinement with Al-5Ti-0.2B additions increased pore sizes and N in 2024 alloy products. Similar results were reported by Fakhraei et al. [25] who observed that as Ti amount increased in the melt, porosity increased in an Al-20%Mg alloy. As an alternative to Ti grain refinement, Al-3B master alloy has been used which produces AlB_2 and B in the melt to act as heterogeneous nucleates for grains [26]. Dispinar et al. [27] investigated the differences in porosity distribution between Ti-B and B grain refinement additions. More localized porosity was observed with B grain refinement compared to the evenly distributed pores with Ti-B grain refinement. Moreover, Schaffer and Dahle [28] and Dispinar et al. [27] observed that Ti tended to sink to the bottom due to its higher density, which is known as fading. With B grain refinement, no fading effect was observed.

Lee et al. [29] investigated the effect of melt treatments including modification by Sr addition and grain refinement with Ti as well as degassing on the porosity and tensile properties in A356 alloy castings. They determined that the Sr and Ti additions increased porosity. However, degassing, with or without other melt treatments, significantly decreased porosity and consequently improved tensile properties. Similar results were found by Haberl et al. [30] who reported almost 50% reduction in N in RPT samples after degassing. Although it is well known that degassing reduces the hydrogen content, the main advantage of degassing is considered to be the floatation of bifilms to the surface of the melt [31].

2.2. Hot tear sensitivity

Hydrostatic tensile stresses are generated in the liquid phase in solidifying castings, which may result in the formation of a pore. Similarly, hot tear is a nucleation-controlled damage process [32] but takes place only when uniaxial tensile stresses are formed in a weak material. There have been a number of studies in which hot tearing sensitivity (HTS) was investigated experimentally and analytically in aluminum alloys [33]. Several studies were conducted using different mold types and different casting parameters to solve this defect. One of these studies was carried out with CRC (constrained rod casting) mold. CRC mold has four different arms that have different arm length, as presented in Fig. 1. Lin et al. [34] investigated hot tearing sensitivity and effect of grain refinement in AA1050, AA3104 and AA5182 alloys. They determined that grain refining reduced hot tearing sensitivity, which is in accordance with findings in other studies [35–42]. However, Warrington et al. [43] observed that excessive additions of grain refiner to 7XXX aluminum alloys increased occurrence of hot tears. Wu et al. [44] studied on hot tearing in A380 aluminum alloy with both unmodified and modified and reported that Sr modification effectively decreased hot tearing. Similar results were reported by Puncreobutr et al. [45] who found that the addition of Sr and/or TiB_2 reduced hot tearing sensitivity in A319 aluminum castings.

In this study, the effect of melt additions and processing on melt quality is characterized first. Then, the link between the initial melt quality and hot tear sensitivity was also established with regard to alloying and melt treatments.

Fig. 1. The mold for the constrained rod casting (CRC) used in this study.

3. Experimental details

Chemical composition of A380.1 alloy that was used in this study is given Table 1. Ingots were cut to be charged into the crucible. A resistance furnace that has 22 kg capacity was used to melt the alloy. Twelve different melts were prepared by using virgin ingots from the same heat. The experimental variables and the levels at which they were tests are outlined in Table 2. In non-degassed melts, grain refinement and modification additions were made once the melt temperature reached 1013 K (740 °C). Master alloys used in this work were Al-Ti5B1, AlSr15 and Al-3B with the chemical compositions given in Table 3. AlTi5B1 and Al3B alloys were added into liquid A356 for grain refinement to obtain a concentration of 10 ppm Ti or 10 ppm B. AlSr15 alloy was added the melt for modification to obtain a concentration 30 ppm. RPT sample collection and pouring castings started after 10 min of holding period.

For degassing process, a T-type graphite lance was used [46]. Degassing process was started when melt temperature reached 1013 K (740 °C) and was carried out for 20 min with argon. Gas flow rate was held at 2 L/min. Master alloy additions were made when the degassing was completed and after the surface of the melt was skimmed.

A sand mold that can take two samples at same time was used to obtain RPT samples in vacuum of 80 mbar [46]. Samples had rectangular shape with height of 55 mm and a thickness of 10 mm. All RPT samples were cut into two vertically (cross section) and one half was prepared with sandpaper for image analysis. In this process, 60, 180, 400 and 600 grid sandpapers were used in sequence. Subsequently, all RPT samples were scanned with 600 dpi resolution. Digital image analysis was conducted on each specimen by following the guidelines provided by Dispinar and Campbell [47] and using SigmaScan software.

After RPT samples were taken, melts were poured into the constraint rod casting (CRC) mold, presented in Fig. 1. Initial mold temperature was held at 220 °C, which was reported by Limmaneevichitr et al. [48] to produce maximum hot tearing sensitivity in aluminum alloys.

Three castings were poured for each condition. Samples were taken from constrained rod castings for microstructural analysis. In addition, fracture surfaces in castings with hot tears were examined via scanning electron microscopy.

4. Results and discussion

The microstructure of samples from degassed samples is presented in Fig. 2. Note that Sr addition reduces the size of Si particles significantly. The dendrite arm spacing (DAS) values measured from micrographs are presented in Note that Ti-B and B additions reduce DAS slightly in both non-degassed and degassed melts.

Table 1
Chemical composition (in wt%) of the alloy used in this study.

Si	Fe	Cu	Mn	Mg	Zn	Ti	B	Al
8.14	0.64	3.12	0.44	0.22	0.49	0.02	0.001	rem.

Table 2
The experimental variables and the levels at which they were tested.

Parameter	Levels
Degassing	No degassing; degassing
Sr addition	0 ppm (unmodified); 30 ppm (modified)
Grain refiner	No addition; AlTi5B1; Al3B;

Table 3
Chemical composition (in wt%) of the master alloys.

Master alloys	Ti	Sr	B	Fe	Si	Ca	Al
AlSr15	–	% 14–15	–	≤% 0.2	≤% 0.2	≤% 0.2	Rem.
AlTi5B1	% 5	–	% 1	≤% 0.2	≤% 0.2	–	Rem.
Al3B	–	–	% 2.5–3.5	% 0.3	% 0.2	–	Rem.

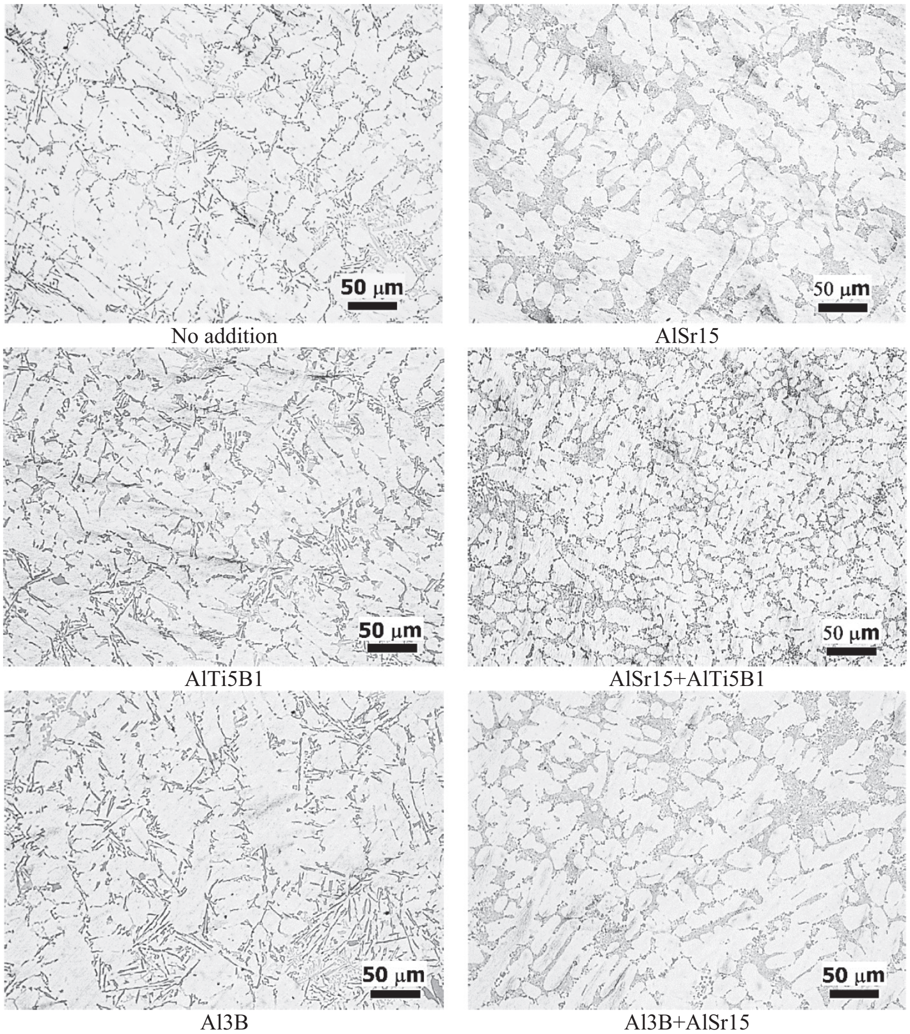

Fig. 2. The microstructure of the castings from various melts.

4.1. Characterization of melt quality

The cross sections of RPT samples are presented in Fig. 3. Differences between degassed and non-degassed samples are clear for all conditions. While varying levels of porosity is evident in non-degassed castings, the number of pores is significantly reduced after

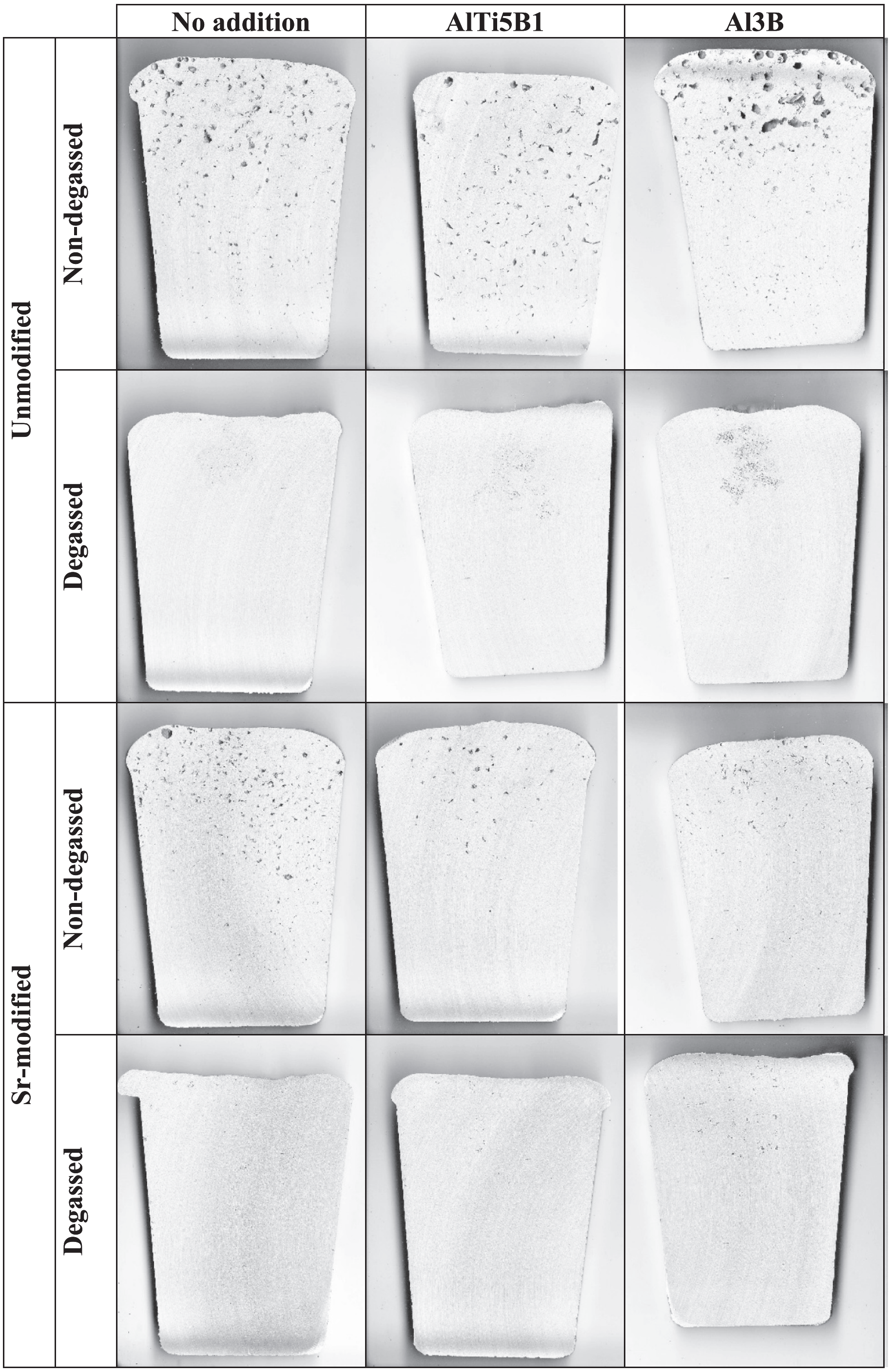

Fig. 3. The cross-section of RPT samples for all melts included in this study.

degassing. This is an indication that rising bubbles during degassing had cleared the old bifilms in the melt.

The number density of pores for all melts is presented in Fig. 4 and Note that AlTi5B1 addition increases N and therefore degrades melt quality when melt is not degassed. After degassing, however, AlTi5B1 addition has no effect on N. When Sr is added, AlTi5B1 additions improve melt quality by reducing N in both non-degassed and degassed melts. Similarly Al3B additions improve melt quality in the presence of Sr. When Sr is not added, Al3B additions impair melt quality. When only Sr is added to the melt without any grain refiners, melt quality is greatly reduced regardless of degassing. All additions damage the molten metal when the metal is not degassed. This is an evidence of “bifilms created by charging through the surface entrainment” as explained by Campbell [2].

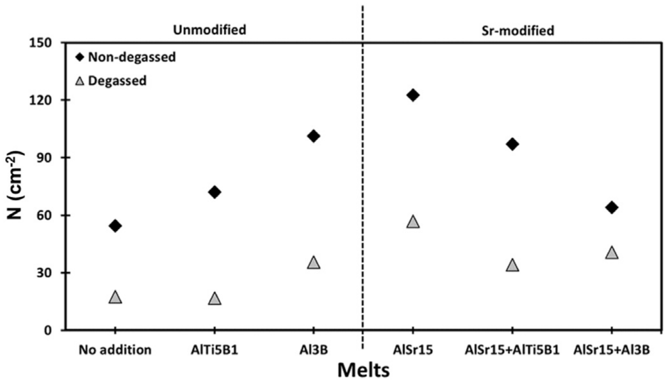

Fig. 4. Number density of pores in RPT samples for all melts.

The size distribution of all pores was analyzed first by calculating the equivalent diameter, d_{eq}, for all pores;

$$d_{eq} = \sqrt{\frac{4A}{\pi}} \tag{1}$$

where A is the area of the pore on the polished surface of the RPT sample. Subsequently, it was hypothesized that d_{eq} followed the lognormal distribution, which is consistent with the theory that pore size distribution in castings should be lognormal [49] as well as observations in Mg [50] and Al [51] alloy castings. The density function (f) for the lognormal distribution is written as;

$$f(d_{eq}) = \frac{1}{d_{eq}\sigma\sqrt{2\pi}} \exp\left[\frac{-(\ln(d_{eq}) - \mu)^2}{2\sigma^2}\right] \tag{2}$$

where σ is the shape and μ is the scale parameter. The expected value, i.e., mean of a lognormal distribution is found by;

$$\overline{d}_{eq} = e^{\mu+\sigma^2/2} \tag{3}$$

Parameters of the lognormal distribution were estimated by using the maximum likelihood method. The goodness-of-fit of the estimated parameters was tested by using the Anderson-Darling statistic [52]. In all cases, the hypothesis that the data come from the fitted lognormal distributions could not be rejected.

The lognormal distributions for “no addition” melts, non-degassed and degassed, are shown in Fig. 5.a. Degassing reduces pore sizes and consequently pore size distribution is shifted to lower sizes. This shift can be at least partially attributed to reduction in H level in the melt that would be expected after degassing with argon. With lower level of dissolved hydrogen in the melt, entrained bifilms would inflate less under reduced pressure, resulting in lower pore sizes.

The estimated parameters and Eq. (3) were used to calculate average pore size for each melt, which are provided in Table 4 and Fig. 5.b. Note that in all cases, except for AlSr15 + AlTiB1, the average pore size is smaller after degassing. In degassed melts, pore sizes become larger after grain refining regardless of the Sr level.

Arnberg et al. [53] who studied grain refinement with B in the absence of Ti and observed more globular dendrites with B additions than when Ti was also present. The results of these two studies can be interpreted together; bifilms are pushed to the center of the casting when B is added, resulting in porosity being concentrated in the center of castings.

4.2. Hot tear sensitivity

The formulation developed by Lin et al. [34] to quantify hot tear sensitivity, HTS, was used in this study;

$$HTS = \sum_{i=1}^{4} (L_i.\ C_i) \tag{4}$$

where L_i is the weight associated with each arm, i.e., 1 for longest arm, increasing by one from bottom to top with 4 for shortest arm, and C_i is the severity of hot tearing, which is zero for no hot tear and 4 for fully detached arm. This formulation gives HTS values between zero and forty. The HTS results are presented in Fig. 6, which shows that HTS values are higher after Sr addition in all cases. The lowest HTS was obtained in degassed melt with Al3B addition and the highest HTS was in degassed melts with Al3B and Sr additions. Castings from these conditions are shown in Fig. 7. It is noteworthy that the degassed melts with Al3B additions that showed no hot tears without Sr became highly susceptible to hot tears after Sr additions. Moreover, Fig. 6 shows that the effect of degassing on HTS depends on whether Sr has been added to the melt. In melts without Sr, degassing reduces HTS. After Sr additions, however, degassing increases HTS. This interaction between degassing and Sr addition has not been reported previously, to the authors' knowledge, and will be discussed in more detail below.

Scanning electron microscopy of hot tear surfaces in non-degassed showed the presence of coarse, “old” bifilms, possibly the skin

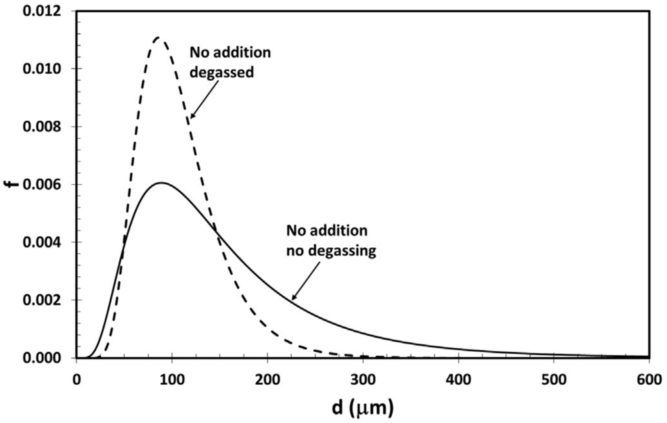

(a)

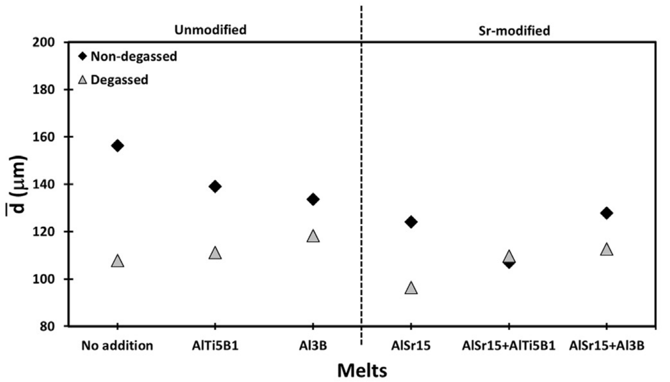

(b)

Fig. 5. Pore size distributions in RPT samples: (a) lognormal distribution fits for two melts with no additions, and (b) averages of lognormal distributions calculated from estimated parameters.

Table 4
Number density and hot-tear sensitivity for all melts.

Degassing	Melts	DAS (μm)	N (cm^{-2})	$\bar{d}_{eq}$ (μm)	HTS
No degassing	No addition	19	54.5	156	6.67
	AlTi5B1	14	72.2	139	6.00
	Al3B	14	101.4	134	1.33
	AlSr15	16	122.6	124	11.00
	AlSr15 + AlTi5B1	16	67.9	107	13.00
	AlSr15 + Al3B	13	64.1	128	11.67
Degassing	No addition	16	17.6	108	3.00
	AlTi5B1	13	16.8	111	0.67
	Al3B	15	35.7	118	0.00
	AlSr15	17	56.8	96	10.33
	AlSr15 + AlTi5B1	15	34.1	110	14.00
	AlSr15 + Al3B	14	40.6	113	14.33

of the ingot, as shown in Fig. 8.a. These old bifilms were not found on hot tear surfaces of degassed castings. In Sr-modified castings, small intermetallic-like features were observed, as presented in Fig. 8.b, which were interpreted as Al_2SrO_3 oxide. These features were not found in unmodified castings, Fig. 8.c.

An attempt was made to determine whether there was a relationship between N and HTS. However, a direct relationship could not be found. This can be attributed to the damage the melt can be expected to receive during pouring and mold filling which would change the quality of the metal at the start of solidification. Assuming that the damage to liquid metal during mold filling would be identical, a comparative approach was taken to determine the effects of the variables in N-HTS correlations. For this comparative approach, the change in HTS, i.e., ΔHTS versus the ratio of N after a given melt treatment (+) to before (−) was used. For instance, to determine the effect of degassing in the "no addition" condition, $\Delta HTS = 3.00–6.67 = -3.67$ and $N_+/N_- = 17.6/54.5 = 0.323$. The

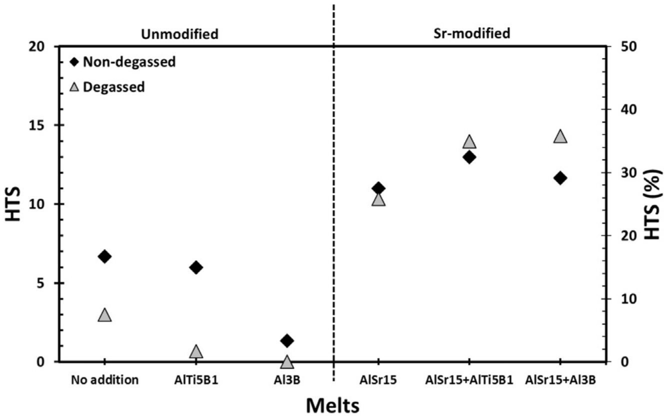

Fig. 6. Hot tear sensitivity for all melts.

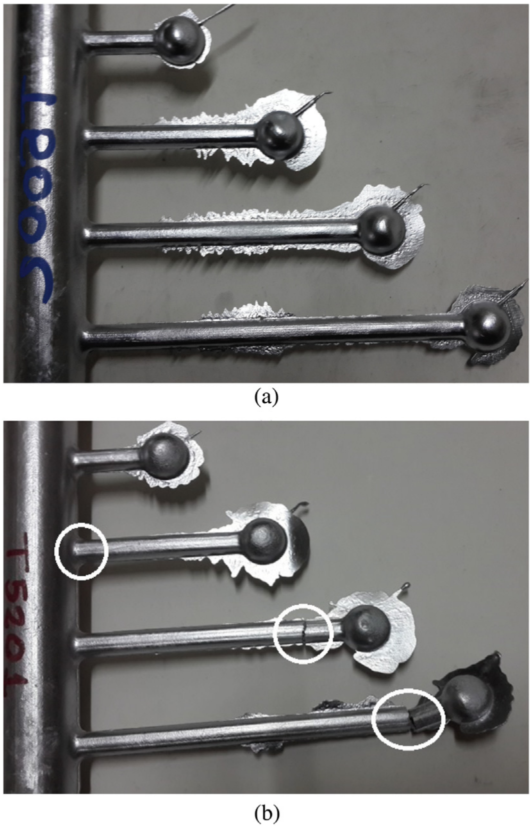

Fig. 7. Hot tear sensitivity in degassed melts with (a) Al3B, and (b) AlSr15 + Al3B additions, representing the best and worst cases, respectively.

results of this analysis for each variable are given below.

4.3. The effect of degassing

The change in HTS versus N-ratio for degassing is presented in Fig. 9. Note that all N ratios are < 1.0, i.e., degassing reduced N, as discussed previously. When data are analyzed this way, a linear relationship between ΔHTS and N_+/N_- is observed. Hot tear tendency is increased when N_+/N_- is higher than approximately 0.5. At N_+/N_- values lower than 0.5, the hot tear sensitivity is reduced. When no addition is made to the liquid metal, degassing reduces hot tear sensitivity by removing the large, coarse bifilms, such as the one in Fig. 8.a. During grain refiner and/or modifier addition to the melt, there is inevitably some damage given to the metal by incorporating the surface of the melt as well as the skin of the master alloy addition [1]. If only grain refiner or modifier is added after degassing, HTS is reduced with respect to non-degassed melts. Assuming that all large old bifilms would be removed

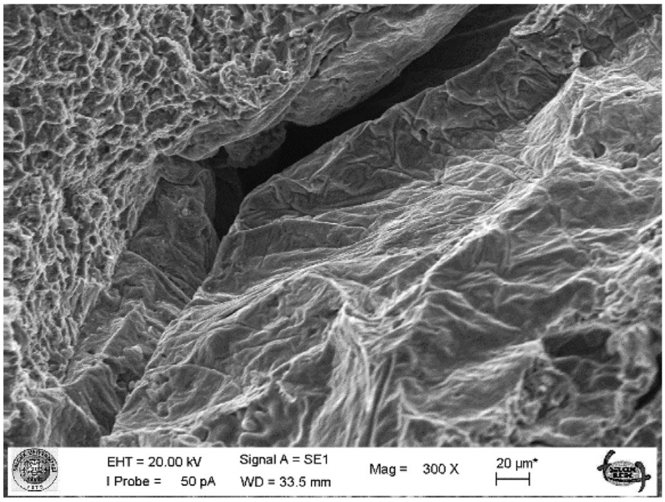

(a)

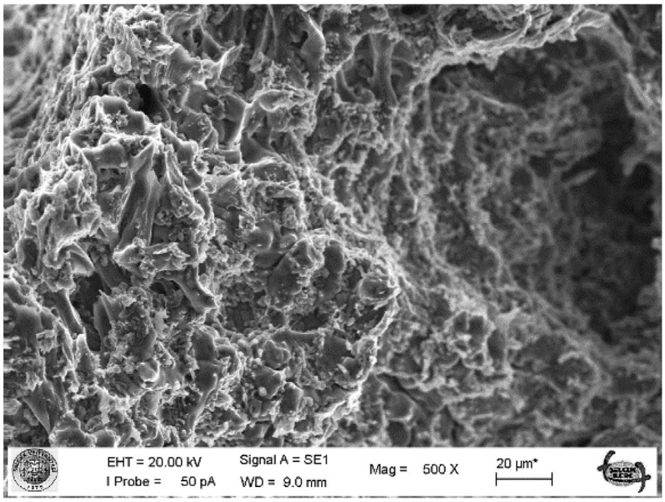

(b)

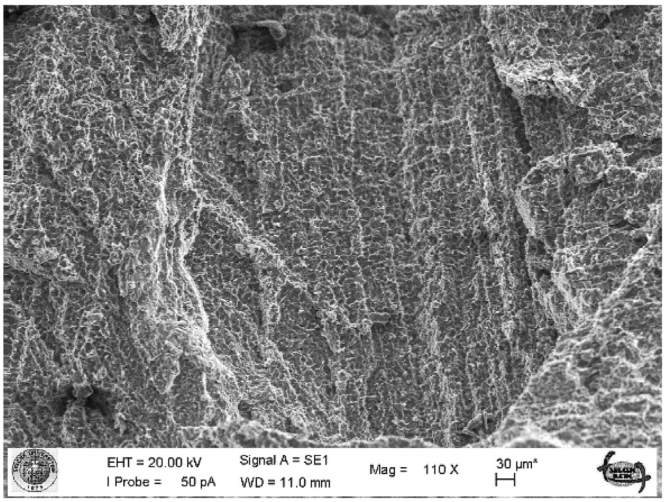

(c)

Fig. 8. Features on hot tear surfaces of (a) non-degassed castings with large old bifilms, (b) Sr-modified castings showing small intermetallic-like particles, and (c) degassed castings with no Sr addition.

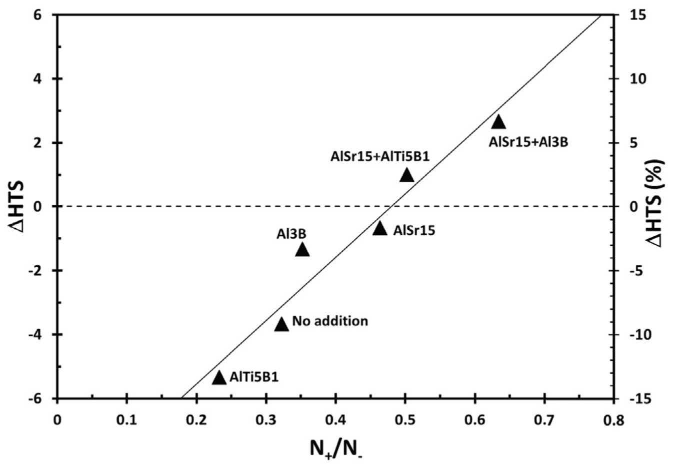

Fig. 9. The effect of degassing with N ratio plotted versus the change in hot tear sensitivity. Every point represents the comparison between degassed (+) and non-degassed (−) melts with other additions.

during degassing, the beneficial effect presented in Fig. 9 can be due to (i) sedimentation of any residual bifilms in the melt before pouring, or (ii) slightly increased bifilm content in the casting that can accommodate the uniaxial thermal stress during solidification better because of opening bifilms without reaching the casting surface. When grain refiner and Sr are added together to a degassed melt, the increase in old bifilm content due to surface entrainment is large enough to have bifilms opening during solidification to reach the casting surface and therefore increasing ΔHTS.

4.4. The effect of Sr-modification

The plot of ΔHTS versus N_+/N_- for Sr-modification is presented in Fig. 10. Note that all ΔHTS values for Sr-modification are positive, indicating that Sr-modification increases hot tear sensitivity regardless of the condition of the melt. These results are in contrast with the findings of Wu et al. [44] and Puncreobutr et al. [45] in Al-Si-Cu-Mg alloys. Also note in Fig. 10 that degassed and non-degassed melts yield separate relationships with similar slopes, and degassed melts yield higher ΔHTS values. The addition of Sr to non-degassed melts with large old bifilms already entrained, increases the number of bifilms in the melt. However, Sr additions were also found to break up the oxides [54,55], such as the ones seen in Fig. 8.b. Because old bifilms can partially accommodate the uniaxial strain during solidification, Sr additions lead to increased HTS at lesser magnitudes in non-degassed melts than in degassed melts. As seen in Figs. 4 and 5, the addition of Sr to the melt decreases pore size and average pore size, whereas number density of pores increases. This indicates that larger bifilms are split into smaller bifilms when oxide structure is altered by spinel formation due to Sr addition. Thus, smaller and higher number of pores are found in the cast part.

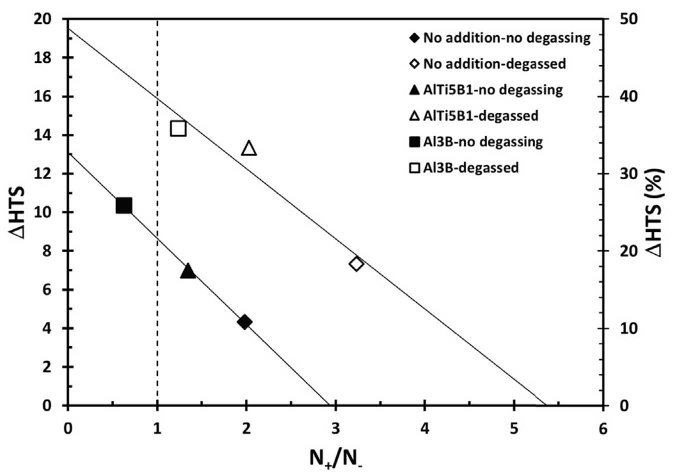

Fig. 10. The effect of Sr addition on the change in HTS with the N-ratio. Data indicated are for the (−) levels.

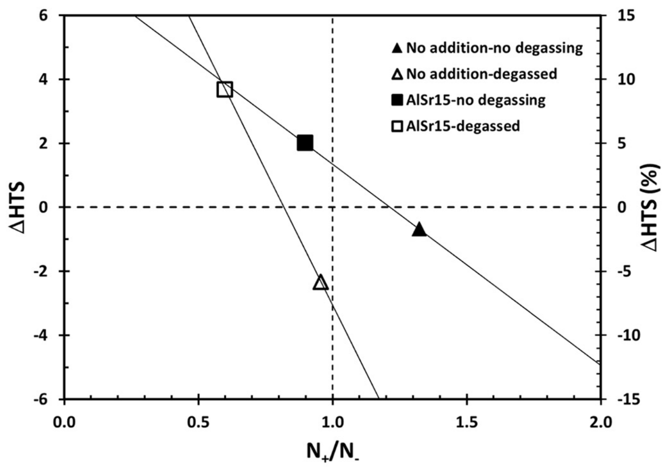

(a)

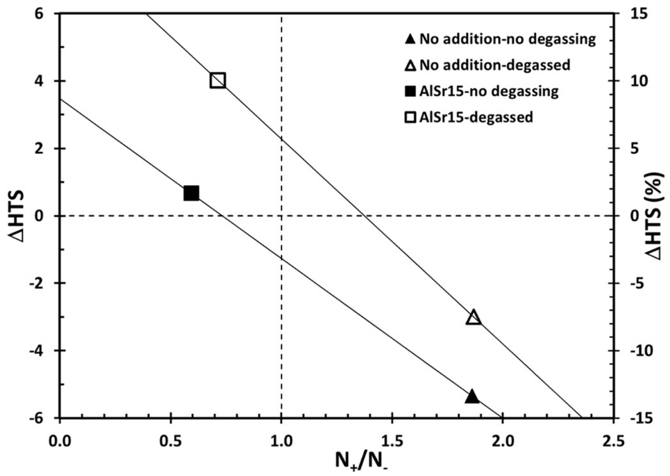

(b)

Fig. 11. The effect of grain refining additions, (a) TiB and (b) B, on the change in HTS with N-ratio. Data indicated are for the (−) levels.

4.5. The effect of grain refinement

The change in ΔHTS with N_+/N_- for grain refinement is presented in Figs. 10 and 11. The effect of both type of grain refiners is generally to increase HTS when they reduce N in RPT samples (N-ratio $<$ 1) and to decrease HTS when N-ratio is larger than 1. This counterintuitive result can only be explained by increased number of bifilms serving to accommodate tensile strains in the constrained rod casting. When less number of bifilms are present, strain is concentrated on the few bifilms which lead to more cracks being observed on the surface of the castings.

The results presented above reiterate what many researchers observed before;

(i) hot tear is a very complex phenomenon, because it is not always seen under the same conditions. Many results in literature show large scatter in their findings.

(ii) the scatter in data may mask true effects of process variables such as melt treatments and additions, and because depending on the cooling conditions, efficiency of gran refinement or modification may vary. The size and distribution of grain refiner may end up in establishment of non-uniform dendritic growth. As a result, columnar growth enhances hot tearing. Thus, it is not easy to conclude that grain refinement decreases hot tearing tendency. Additionally, hydrostatic tensions in liquid metal is so strong, it should take the shape of the geometry that it is in [50]. Thus, for a liquid to separate into two, a heterogeneous nucleant is required. In the case of aluminum alloys, the non-bonded folded faces of oxides (i.e. bifilms) can easily initiate such cracks in liquid [51].

(iii) bifilms play a major role in hot tear [55,56].

5. Conclusions

- Hot tear is a complex phenomenon. There is no single parameter that can be eradicated to be pin down as the source for hot tearing. There are too many parameters that need to be controlled and defined. Nevertheless, it has been found that in aluminum alloys, the most deleterious defects, bifilms that are the cause of many defects, play an important role in initiating the hot tearing during solidification.
- The shape, size and distribution of bifilms both in melt and in the cast part are too complex. They can be in many forms and sizes. They may come from the melt. They may also be generated during filling of the mold. The transport phenomena and fluid flow analysis are not accurate enough to simulate how bifilms can float in the melt. It is not easy to locate where they may end up in the mold cavity. Therefore, it makes it more difficult to estimate whether a hot tearing can occur or not. Nevertheless, they act as heterogeneous nucleation site for liquid to separate and thus increases hot tearing.
- Sr additions coupled with grain refining increases HTS. The change in HTS from no degassing to degassed melt is increased by 5% when either Ti or B is added to melt.
- Best quality melt is obtained after when A380 was grain refined by Al3B even when melt was not degassed.
- Best HTS is obtained in degassed melts with Al3B addition which was zero. The extrapolation of data indicates that when number density of pores are decreased in Al3B addition, HTS reaches a negative value which shows that Al3B is the best means of eliminating hot tearing tendency in A380 alloy.
- Pore size and average pore decreases when melt is modified by Sr. However, number of pores increases. This indicates that Sr breaks up oxide inclusion.

Acknowledgements

This work has been supported by the Scientific Research Projects Coordination Unit of Selcuk University (Project number: 13101026). Author would like to thanks to TUBITAK (1059B141401190) (Turkey) for its supporting.

References

[1] J. Campbell, Entrainment defects, Mater. Sci. Technol. 22 (2) (2006) 127–145.
[2] J. Campbell, Complete Casting Handbook: Metal Casting Processes, Metallurgy, Techniques and Design, Elsevier Science, 2015.
[3] L. Katgerman, D.G. Eskin, In search of prediction of hot cracking in aluminium alloys, in: H.H. Thomas Bollinghaus, Carl E. Cross, John C. Lippold (Eds.), Hot Cracking Phenomena in Welds II, Springer, Berlin, 2008, pp. 3–18.
[4] R. Harris, S. Lipson, H. Rosenthal, Tensile properties of aluminum–silicon magnesium alloys and the effect of sodium modification, AFS Trans. 64 (1956) 470–481.
[5] J.E. Gruzleski, B.M. Closset, The Treatment of Liquid Aluminum-silicon Alloys, (1990).
[6] S. Shivkumar, et al., An experimental study to optimize the heat treatment of A356 alloy, AFS Trans. 97 (1989) 791–810.
[7] M. Drouzy, S. Jacob, M. Richard, Interpretation of tensile results by means of quality index and probable yield strength-application to Al-Si7 mg foundry alloys-France, Int. Cast Metals J. 5 (2) (1980) 43–50.
[8] M. Uludağ, et al., The effect of Sr modification and holding time on Si morphology and mechanical properties of ETIAL 195 alloy, Pamukkale Univ. J. Eng. Sci. 21 (8) (2015) 348–351.
[9] Q. Fang, D. Granger, Porosity formation in modified and unmodified A356 alloy castings, AFS Trans. 97 (10) (1989) 989–1000.
[10] G. Byczynski, D. Cusinato, The effects of strontium and grain refiner additions on the fatigue and tensile properties of industrial Al-Si-Cu-Mg alloy castings produced using the Ford Motor Company—Cosworth precision sand process, Int. J. Cast Metals Res. 14 (5) (2002) 315–324.
[11] M. Brosnan, S. Shivkumar, Elevated-temperature Tensile Properties and Fracture Behavior of A 356 Castings, American Foundrymen's Society, Inc, USA, 1996, pp. 727–737.
[12] R. Gundlach, et al., Thermal fatigue resistance of hypoeutectic aluminum-silicon casting alloys (94–141), Transac. Am. Foundrymen's Soc. 102 (1994) 205–224.
[13] J. Campbell, M. Tiryakioğlu, Review of effect of P and Sr on modification and porosity development in Al–Si alloys, Mater. Sci. Technol. 26 (3) (2010) 262–268.
[14] H. Iwahori, et al., Occurring behavior of porosity and feeding capabilities of sodium-and strontium-modified Al-Si alloys, AFS Trans. 98 (1990) 167–173.
[15] M. Uludağ, et al., On the interpretation of melt quality assessment of A356 aluminum alloy by the reduced pressure test: the Bifilm index and its physical meaning, Int. J. Met. (2018) 1–8.
[16] D. Argo, J. Gruzleski, Porosity in modified aluminum alloy castings, AFS Trans. 96 (1988) 65–74.
[17] C. Dinnis, et al., The influence of strontium on porosity formation in Al-Si alloys, Metall. Mater. Trans. A 35 (11) (2004) 3531–3541.
[18] N.S. Tiedje, J.A. Taylor, M.A. Easton, Feeding and distribution of porosity in cast Al-Si alloys as function of alloy composition and modification, Metall. Mater. Trans. A 43 (12) (2012) 4846–4858.
[19] N.S. Tiedje, J.A. Taylor, M.A. Easton, A new multi-zone model for porosity distribution in Al–Si alloy castings, Acta Mater. 61 (8) (2013) 3037–3049.
[20] L. Hengcheng, et al., Effect of Sr content on porosity formation in directionally solidified Al-12.3 wt.% Si alloy, China Foundry 11 (5) (2014).
[21] N. Roy, et al., Porosity formation in Al-9 wt% Si-3 wt% Cu-X alloy systems: measurements of porosity, J. Mater. Sci. 31 (5) (1996) 1243–1254.
[22] L. Liu, et al., Influence of oxides on porosity formation in Sr-treated Al-Si casting alloys, J. Mater. Sci. 38 (6) (2003) 1255–1267.
[23] M. Mostafaei, et al., Evaluation of the effects of rotary degassing process variables on the quality of A357 aluminum alloy castings, Metall. Mater. Trans. B Process Metall. Mater. Process. Sci. 47 (6) (2016) 3469–3475.
[24] P.N. Anyalebechi, Hydrogen-induced gas porosity formation in Al–4.5 wt% Cu–1.4 wt% Mg alloy, J. Mater. Sci. 48 (15) (2013) 5342–5353.
[25] O. Fakhraei, M. Emamy, H. Farhangi, The effect of Al–5Ti–1B grain refiner on the structure and tensile properties of Al–20% Mg alloy, Mater. Sci. Eng. A 560 (2013) 148–153.
[26] L. Yuan, D. Chao, Y.-X. Li, Grain refining mechanism of Al-3B master alloy on hypoeutectic Al-Si alloys, Trans. Nonferrous Metals Soc. China 21 (7) (2011) 1435–1440.
[27] D. Dispinar, et al., Degassing, hydrogen and porosity phenomena in A356, Mater. Sci. Eng. A 527 (16) (2010) 3719–3725.
[28] P.L. Schaffer, A.K. Dahle, Settling behaviour of different grain refiners in aluminium, Mater. Sci. Eng. A 413 (2005) 373–378.
[29] J.-M. Lee, et al., Effects of melt treatments on microstructures and mechanical properties of A357 alloy, J. Korea Foundry Soc. 23 (2) (2003) 69–76.
[30] K. Haberl, et al., Characterization of the melt quality and impurity content of an LM25 alloy, Metall. Mater. Trans. B Process Metall. Mater. Process. Sci. 40 (6) (2009) 812.
[31] J. Campbell, Metallurgy without bifilms: no more fractures, Shape Casting: 5th International Symposium 2014, John Wiley & Sons, Inc., 2013.
[32] J. Campbell, Complete Castings Handbook, Butterworth-Heinemann, Oxford, 2011.

[33] Y.F. Guven, J.D.H., Hot-tearing in aluminium copper alloys, Cast Metals 1 (2) (1988) 104–111.
[34] S. Lin, C. Aliravci, M.O. Pekguleryuz, Hot-tear susceptibility of aluminum wrought alloys and the effect of grain refining, Metall. Mater. Trans. A 38 (5) (2007) 1056–1068.
[35] M. Easton, et al., An analysis of the effect of grain refinement on the hot tearing of aluminium alloys, Mater. Forum 28 (2004) 224–229.
[36] M. Fortier, et al., Mold surface roughness effects on the microstructure and the hot tearing strength for an Al-4.5% Wt Cu alloy, Light Metals (2001) 839–846.
[37] S. Li, Hot tearing in cast aluminum alloys: measures and effects of process variables, Materials Science and Engineering, Worcester Polytechnic Institute, 2010.
[38] S. Metz, M.C. Flemings, Fundamental Study of Hot Tearing, (1970).
[39] R.A. Rosenberg, M.C. Flemings, H.F. Taylor, Nonferrous binary alloys hot tearing, AFS Trans. 69 (1960) 518–528.
[40] M. Sadayappan, et al., Effect of melt processing and magnetic field on the hot tearing of Al-Cu Alloy A 201, Transactions of the American Foundry Society and the One Hundred Sixth Annual Casting Congress, 2002.
[41] M. Easton, et al., The effect of grain refinement and cooling rate on the hot tearing of wrought aluminium alloys, Materials Science Forum, Trans Tech Publ., 2006.
[42] M. Uludağ, et al., Effect of degassing and grain refinement on hot tearing tendency in Al8Si3Cu alloy, Int. J. Met. (2017) 1–7.
[43] D. Warrington, D. McCartney, Hot-cracking in aluminium alloys 7050 and 7010-a comparative study, Cast Metals 3 (4) (1991) 202–208.
[44] Q. Wu, Study of Hot Tearing in Cast and Wrought Aluminum Alloys, Worcester Polytechnic Institute, 2012.
[45] C. Puncreobutr, et al., Influence of Fe-rich intermetallics on solidification defects in Al–Si–Cu alloys, Acta Mater. 68 (2014) 42–51.
[46] D. Dispinar, J. Campbell, Porosity, hydrogen and bifilm content in Al alloy castings, Mater. Sci. Eng. A 528 (10) (2011) 3860–3865.
[47] D. Dispinar, J. Campbell, Reduced pressure test (RPT) for bifilm assessment, Shape Casting: 5th International Symposium 2014, John Wiley & Sons, Inc., 2013.
[48] C. Limmaneevichitr, A. Saisiang, S. Chanpum, The role of grain refinement on hot crack susceptibility of aluminum alloy permanent mold castings, Proceedings of the 65th World Foundry Congress, 2002.
[49] H. Dvorak, E. Schwegtier, Statistical distribution of flaw sizes, Int. J. Fract. Mech. 8 (1) (1972) 110–111.
[50] M. Tiryakioğlu, Pore size distributions in AM50 Mg alloy die castings, Mater. Sci. Eng. A 465 (1) (2007) 287–289.
[51] M. Tiryakioğlu, On fatigue life variability in cast Al–10% Si–Mg alloys, Mater. Sci. Eng. A 527 (6) (2010) 1560–1564.
[52] T.W. Anderson, D.A. Darling, A test of goodness of fit, J. Am. Stat. Assoc. 49 (268) (1954) 765–769.
[53] L. Arnberg, L. Bäckerud, H. Klang, 1: production and properties of master alloys of Al–Ti–B type and their ability to grain refine aluminium, Metals Technol. 9 (1) (1982) 1–6.
[54] M. Uludağ, et al., Characterization of the effect of melt treatments on melt quality in Al-7wt %Si-Mg alloys, Metals 7 (5) (2017) 157.
[55] M. Uludağ, R. Çetin, D. Dispinar, Freezing range, melt quality, and hot tearing in Al-Si alloys, Metal. Mater. Trans. A (2018) 1–14.
[56] M. Uludağ, R. Çetin, D. Dışpınar, Observation of hot tearing in Sr-B modified A356 alloy, Archiv. Foundry Eng. 17 (4) (2017) 165–168.